ELectronics EXpress

IEICE Electronics Express, Vol.16, No.11, 1–6

LETTER

Enhanced resonance transmission of a small square aperture loaded with parallel wires in a ground plane

Ki-Chai Kim[1a)] and Young-Ki Cho[2b)]

Abstract This paper presents the resonance transmission of a small, square aperture with two parallel wires in a ground plane. When a plane wave excites a square aperture, aperture resonance occurs using parallel wires, which is known as resonance transmission or maximum power transmission. The resonant frequency of a 3-cm square aperture structure was reduced from 4.18 GHz to various desired frequencies by adding wires. The enhanced transmission cross sections using two parallel wires were $\approx 3\lambda^2/4\pi$ ($= 2G\lambda^2/4\pi$, $G = 1.5$) for square widths of $\lesssim 0.22\lambda$, and approached $3.56\lambda^2/4\pi$ ($= 2G\lambda^2/4\pi$, $G = 1.78$) for square widths $\gtrsim 0.22\lambda$. The small square aperture enhanced transmission cross sections using parallel wires were between $3\lambda^2/4\pi$ and $3.56\lambda^2/4\pi$.

Keywords: electrically small square aperture, resonance transmission, enhanced resonance transmission, parallel wires, transmission cross section

Classification: Microwave and millimeter-wave devices, circuits, and modules

1. Introduction

The penetration of electromagnetic fields and wave transmission through a slot aperture in a conducting screen have been extensively studied [1, 2, 3, 4, 5, 6, 7, 8, 9, 10, 11, 12, 13, 14, 15, 16]. The reduction problem of the electromagnetic field penetration through a half-wavelength narrow slot has been investigated in the electromagnetic compatibility (EMC) fields as an aperture cutoff filter [17, 18]. A very small number of electromagnetic waves are transmitted through small slots. To obtain a high transmission efficiency for an electrically small aperture, resonance transmission is obtained by placing a capacitor across the midpoint of the aperture [19] and by deforming the aperture shape [20, 21, 22, 23, 24, 25, 26, 27, 28, 29].

This paper investigates the resonance transmission phenomenon to obtain a high transmission for an electrically small square aperture as an aperture pass filter. The resonance transmission through a small, square slot occurs when two parallel wires are installed on a square aperture. The integral equation for the magnetic current of the square aperture was derived and solved by applying Galerkin's method of moments (MoM). When a plane wave excites a square aperture, the aperture magnetic current can be controlled by the two parallel wires, and the resonance transmission (maximum power transmission) occurs at a given frequency. In this paper, such resonance transmission is called *enhanced resonance transmission*.

The results show that the maximum power transmission of the penetrated electromagnetic power is effectively obtained using the two parallel wires on the small square aperture (SSA). By adding the wires, the resonant frequency of the 3-cm aperture-loaded square structure can be reduced from 4.18 GHz to various desired frequencies of 1 GHz (76.1%), 1.5 GHz (64.1%), and 2 GHz (52.2%). The enhanced transmission cross section (TCS) of the SSA loaded with parallel wires at forced resonance becomes $3\lambda^2/4\pi$ ($= 2G\lambda^2/4\pi$, $G = 1.5$) when the square width is $\lesssim 0.22\lambda$, while the enhanced TCS approaches $3.56\lambda^2/4\pi$ ($= 2G\lambda^2/4\pi$, $G = 1.78$) when the square width is $\gtrsim 0.22\lambda$. However, if the square width is $\approx 0.22\lambda$, the cross section is $3.28\lambda^2/4\pi$ ($G = 1.64$), similar to a half-wavelength resonance narrow slot. The results demonstrate that the enhanced TCS of the SSA using two parallel wires has a value between $3\lambda^2/4\pi$ and $3.56\lambda^2/4\pi$. To verify the theoretical analysis, the calculated transmission cross sections were compared to experiment values.

2. Theoretical analysis

Fig. 1 shows the geometry of an infinitely large ground plane with a small, rectangular aperture. Fig. 1(a) shows the SSA without the two parallel wires, and Fig. 1(b) shows the SSA with the two parallel wires of length h. The parallel wires are parallel to the z-axis and are connected along the x-axis by a distance d. The problem can be divided into two regions that are free space. Region I ($z < 0$) is defined as the half-space containing the incident plane wave $\bar{E}^i$ bounded by the conducting plane. The incident electromagnetic fields transmit into Region II ($z > 0$) through the SSA. We assumed that the square aperture width a is much smaller than the wavelength. In this case, the SSA of a width a is approximately equivalent to a small circular aperture of diameter a. Only the SSA is discussed in this paper.

The unknown aperture magnetic current is $\bar{M} = \hat{z} \times \bar{E}_a$, where $\bar{E}_a$ is the aperture electric field. If a plane wave is incident on the square aperture, the integral equation for the unknown aperture magnetic current in the square aperture can be written as:

[1]Dept. of Electrical Engineering, Yeungnam University, 214–1 Daedong, Kyongsan, Kyongbuk 38541, Korea
[2]School of Electronics Engineering, Kyungpook National University, 80 Daehakro, Bukgu, Daegu 41566, Korea
a) kckim@ynu.ac.kr
b) ykcho@ee.knu.ac.kr

DOI: 10.1587/elex.16.20190269
Received April 22, 2019
Accepted April 24, 2019
Publicized May 14, 2019
Copyedited June 10, 2019

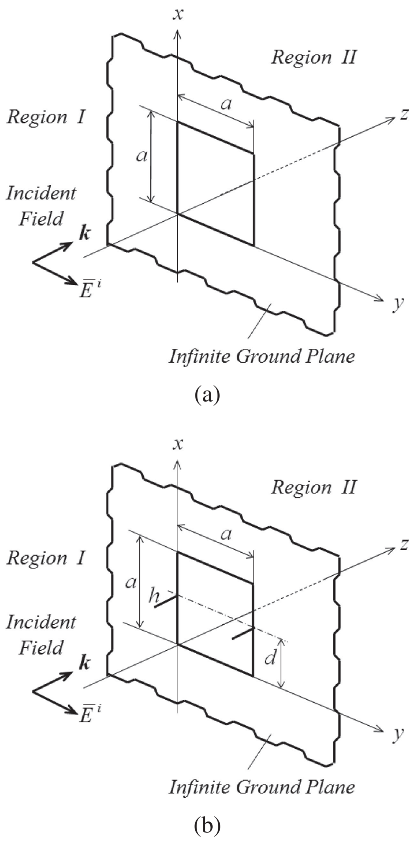

Fig. 1. (a) Small, square aperture and (b) square aperture with two parallel wires in the planar infinite ground plane.

$$\hat{z} \times \left\{ \frac{1}{j\omega\mu_0} \iint_{S'} (\bar{\bar{I}}k^2 + \nabla\nabla) \cdot \bar{\bar{G}}_m^{I}(\bar{r}, \bar{r}') \cdot \bar{M} dS' + \frac{1}{j\omega\mu_0} \iint_{S'} (\bar{\bar{I}}k^2 + \nabla\nabla) \cdot \bar{\bar{G}}_m^{II}(\bar{r}, \bar{r}') \cdot \bar{M} dS' \right\} = \begin{cases} \hat{z} \times (-\bar{H}_{SC}) & \text{for Fig. 1(a)} \\ \hat{z} \times \{-\bar{H}_{SC} - \hat{y} I_y \delta(x-d)\} & \text{for Fig. 1(b)} \end{cases} \tag{1}$$

where $\bar{\bar{I}}$ is a unit dyadic, $\delta(\cdot)$ is the Dirac delta-function, $k = \omega\sqrt{\varepsilon_0\mu_0}$, and ω represents the angular frequency. The superscripts I and II denote the corresponding regions. $\hat{y}$ and $\hat{z}$ are unit vectors in the y and z directions, respectively. The position vectors $\bar{r}$ and $\bar{r}'$ correspond to the observation and source points, respectively. dS denotes an area element on the square aperture, and $\bar{\bar{G}}_m^{I}$ and $\bar{\bar{G}}_m^{II}$ are the dyadic Green functions of the half-space. The time dependence $\exp(j\omega t)$ is assumed and omitted throughout this paper.

In Eq. (1), the incident magnetic field and current at the connecting position of the two parallel wires can be expressed as follows.

$$\bar{H}_{SC} = -\hat{x}\frac{2}{\eta}E_{0y}^{i} \tag{2}$$

$$I_y = \frac{V_L}{Z_L} = \frac{V_L}{-j120\ln\left(\frac{\mathrm{s}}{\mathrm{r}} + \sqrt{\left(\frac{\mathrm{s}}{\mathrm{r}}\right)^2 - 1}\right)\cot(\beta h)} \tag{3}$$

Here, $\bar{H}_{SC}$ is the short-circuited magnetic field when the square aperture is covered by a conducting plate, E_{0y}^{i} is the amplitude of the incident electric field, η is the wave impedance of free space, V_L is the voltage of the wire loading point, Z_L is the impedance of the two parallel wires, and β is the propagation constant of the wires. s $(= a/2 + r)$ and r denote the half-spacing and radius of the wires, respectively.

To solve the simultaneous integral equations for the unknown variables, the aperture electric field, $\bar{E}_a$, is expanded as follows:

$$\bar{E}_a(x, y) = \hat{x}E_{ax}(x, y) + \hat{y}E_{ay}(x, y) = \hat{x}\sum_{p=0}^{P}\sum_{q=1}^{Q} e_{xpq}\cos\frac{p\pi x}{a}\sin\frac{q\pi y}{b} + \hat{y}\sum_{p=1}^{P}\sum_{q=0}^{Q} e_{ypq}\sin\frac{p\pi x}{a}\cos\frac{q\pi y}{b} \tag{4}$$

where e_{xpq} and e_{ypq} are complex expansion coefficients to be determined. In Eq. (4), $E_{ax}(x, y)$ and $E_{ay}(x, y)$ are the cross (cross-polarized component) and dominant (principal component) aperture electric fields, respectively. The dominant aperture electric field, $E_{ay}(x, y)$, consists of an x-dependent dominant field $E_{ay}(x)$ (E_{ay}-field along a line parallel to the x-axis), and a y-dependent dominant field $E_{ay}(y)$ (E_{ay}-field along a line parallel to the y-axis). Substituting the assumed aperture electric field from Eq. (4) into the integral equation, Eq. (1), and employing Galerkin's MoM, yields a linear equation.

When a plane wave excites the square aperture, the transmission coefficient (TC) of the square aperture is defined as follows:

$$TC = \frac{P_{tra}}{P_{inc}} \tag{5}$$

where P_{tra} is the average power transmitted through the aperture, and P_{inc} is the average power incident on the aperture:

$$P_{inc} = Re\left\{\iint_S \bar{E}^i \times \bar{H}^i \cdot \hat{z}dS\right\} = \eta A|H_{0x}^{i}|^2 \tag{6}$$

$$P_{tra} = Re\left\{\iint_S \bar{E}_a \times \bar{H}^* \cdot \hat{z}dS\right\} = Re\left\{\iint_S E_{ax}H_y^* dS\right\} + Re\left\{-\iint_S E_{ay}H_x^* dS\right\} = P_{tra}^{(1)} + P_{tra}^{(2)} \tag{7}$$

where A is the area of the aperture, the asterisk denotes complex conjugation, and H_{Ox}^{i} is the incident magnetic field. The first and second terms, $P_{tra}^{(1)}$, and $P_{tra}^{(2)}$, are the cross and principal components of the transmission power, respectively.

When a plane wave excites the SSA, the TCS of the aperture is defined as the area for which the incident wave contains the power transmitted by the aperture. It follows that TCS is equal to $TC \times A$.

$$
\begin{aligned}
TCS = TC \times A &= \frac{P_{tra}}{\eta |H_{0x}^{i}|^{2}} \\
&= \frac{P_{tra}^{(1)}}{\eta |H_{0x}^{i}|^{2}} + \frac{P_{tra}^{(2)}}{\eta |H_{0x}^{i}|^{2}} \\
&= TCS^{(1)} + TCS^{(2)} \quad \mathrm{m}^2
\end{aligned}
\tag{8}
$$

For a small electrically thin antenna, the maximum absorption area (transmission cross section) is equal to $3\lambda^2/4\pi$ ($= 2G\lambda^2/4\pi$, $G = 1.5$) and is a Hertzian source. If the thin dipole or narrow slot resonates at near half the wavelength, the TCS becomes $3.28\lambda^2/4\pi$ ($= 2G\lambda^2/4\pi$, $G = 1.64$). In general, a square aperture resonates at $a = 0.418\lambda$, and the directive gain is 1.78 [$= 0.81a^2(4\pi/\lambda^2)$] for a conventional TE_{10}-mode aperture field [30]. In this case, the TCS of the square aperture is $3.56\lambda^2/4\pi$ ($= 2G\lambda^2/4\pi$, $G = 1.78$). There is gain difference of 0.14 between the three gains; 1.50, 1.64, and 1.78.

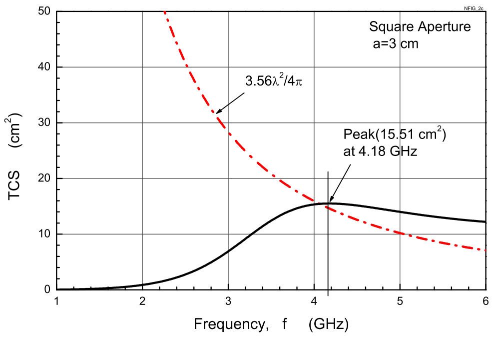

Fig. 2. Frequency characteristics of transmission cross sections for the square aperture without loading reactance: $a = 3$ cm.

Table I. Comparison of the desired and calculated TCS values by MoM.

a (cm)	f (GHz)	a/λ	TCS (cm^2)		
			MoM	$3.56\lambda^2/4\pi$	Within %
1.0	12.5	0.417	1.723	1.632	5.3
2.0	6.27	0.418	6.892	6.486	5.9
3.0	4.18	0.418	15.51	14.59	5.9
4.0	3.13	0.417	27.57	26.03	5.6

For an electrically SSA, the number of waves transmitted through a small square aperture is very small. This paper explains why the enhanced TCS of the SSA with two parallel wires has a value between $3\lambda^2/4\pi$ and $3.56\lambda^2/4\pi$. The effects of two parallel wires on the total TCS ($= TCS^{(1)} + TCS^{(2)}$) is demonstrated here.

3. Transmission cross section of small square aperture

The width of the square aperture is $a = 3$ cm. Frequencies of 1, 1.5, 2, and 3 GHz are used to consider the total TCS of the SSA. The SSA used in the calculation is small compared to the wavelength.

Fig. 2 shows the TCS for a square aperture of $a = 3$ cm without two parallel wires [Fig. 1(a)]. As shown in Fig. 2, the maximum transmission ($TCS = 15.51$ cm^2) for $a = 3$ cm occurs at the resonant frequency 4.18 GHz. Since the directive gain of the square aperture is 1.78 at $a = 0.418\lambda$ (resonance width), the TCS of the square aperture is $3.56\lambda^2/4\pi$ ($= 2G\lambda^2/4\pi$, $G = 1.78$). For the square apertures with $a = 1$ and 3 cm, the desired TCSs ($= 3.56\lambda^2/4\pi$) are 1.632 and 14.59 cm^2, respectively. These desired TCSs and the calculated TCS from Eq. (8) by the MoM differ by only 5.9%, as shown in Table I. However, the TCS is very small at low frequencies, as shown in Fig. 2: $TCS = 0.04$, 0.23, and 0.88 cm^2 at 1.0, 1.5, and 2.0 GHz, respectively. These results demonstrate that the resonance transmission (or maximum transmission) for a SSA with $a = 3$ cm at these frequencies can be effectively obtained using two parallel wires.

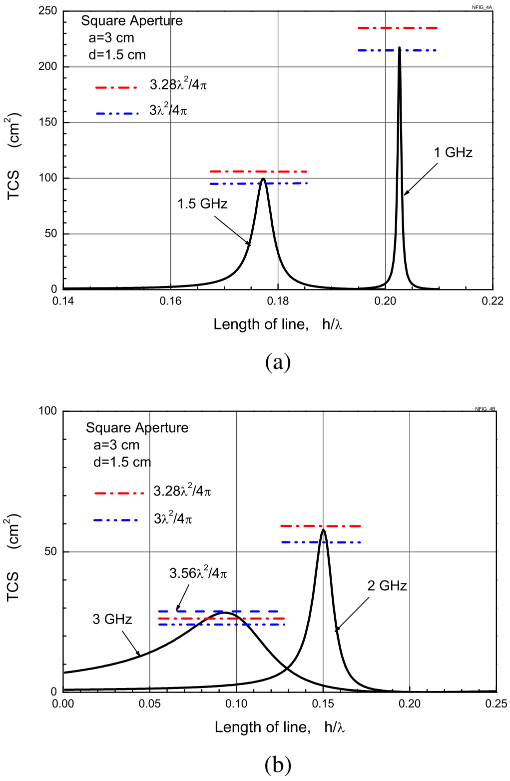

Fig. 3. Transmission cross sections versus length of the two parallel wires for the wire position $d = 1.5$ cm at 1, 1.5, 2, and 3 GHz.

Fig. 3 shows the enhanced TCS of the SSA versus the length of the two parallel wires for the wire position $d = 1.5$ cm (the SSA center) when plane waves of frequencies 1.0, 1.5, 2.0, and 3 GHz are incident on the SSA. The resonance transmissions (maximum transmissions) occur at $h = 0.2026\lambda$ ($= 6.078$ cm), 0.1772λ ($= 3.544$ cm), 0.1500λ ($= 2.250$ cm), and 0.093λ ($= 0.930$ cm), for 1.0, 1.5, 2.0, and 3.0 GHz, respectively, when the wires are connected at $d = 1.5$ cm (the SSA center). This resonance transmission is called enhanced resonance transmission.

The enhanced TCS for the case with parallel wires produces a resonance transmission (either a maximum or enhanced resonance transmission). From Figs. 3(a) and 3(b), the following conclusions can be made. When the size of the square aperture is fixed, the enhanced TCS using parallel wires is close to $3\lambda^2/4\pi$ at lower frequencies [at

1 GHz ($a = 0.1\lambda$) and 1.5 GHz ($a = 0.15\lambda$)]. In this case, the SSA appears to be a Hertzian source at the lower frequency. However, for 2 GHz ($a = 0.2\lambda$), the enhanced TCS using parallel wires is close to $3.28\lambda^2/4\pi$. In this case, the SSA corresponds to a half-wavelength resonant source. The enhanced TCS using parallel wires approaches $3.56\lambda^2/4\pi$ for 3 GHz ($a = 0.3\lambda$). In this case, the SSA corresponds to a resonant rectangular aperture source.

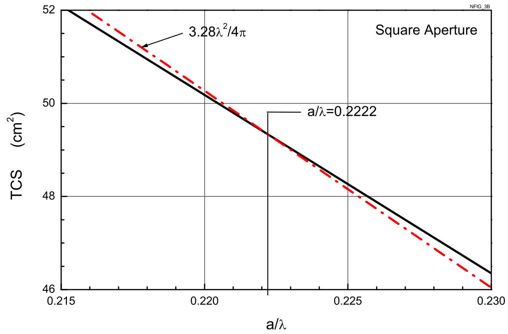

Fig. 4. Transmission cross section versus square aperture width during enhanced resonance transmission.

For 1 and 1.5 GHz, the enhanced TCS approaches $3\lambda^2/4\pi$ ($G = 1.5$), as shown in Fig. 3(a). However, the enhanced TCS approaches $3.28\lambda^2/4\pi$ ($G = 1.64$) at 2 GHz and $3.56\lambda^2/4\pi$ ($G = 1.78$) at 3 GHz, as shown in Fig. 3(b). Therefore, the enhanced TCS of the SSA at forced resonance has a value between $3\lambda^2/4\pi$ and $3.56\lambda^2/4\pi$.

In Fig. 4, when enhanced resonance transmission occurs, the transition boundary of the square width that determines whether the enhanced TCS is closer to $3\lambda^2/4\pi$ ($G = 1.5$) or $3.56\lambda^2/4\pi$ ($G = 1.78$) based on $3.28\lambda^2/4\pi$ ($G = 1.64$). As shown in Fig. 4, the square width of $a = 0.2222\lambda$ is the reference width.

From Figs. 4 and 5, the enhanced TCS of the SSA using two parallel wires is closer to $3\lambda^2/4\pi$ ($G = 1.5$) if the square width is less than 0.2222λ, while the enhanced *TCS* of the SSA by the wires is closer to $3.56\lambda^2/4\pi$ ($G = 1.78$) if the square width is greater than 0.2222λ. When the square width is 0.2222λ, the enhanced TCS has $3.28\lambda^2/4\pi$ ($G = 1.64$). Therefore, $a = 0.2222\lambda$ is the transition boundary of the square width, and the enhanced TCS of the SSA using parallel wires has a value between $3\lambda^2/4\pi$ and $3.56\lambda^2/4\pi$. In this paper, 0.2222λ is approximated to 0.22λ.

Fig. 5 shows the frequency characteristics of the enhanced TCS for a 3 cm SSA width when two parallel wires of length 6.078, 3.544, 2.250, and 0.930 cm for 1, 1.5, 2, and 3 GHz, respectively, are connected at $d = 1.5$ cm. The label "original square aperture" corresponds to the TCS when no parallel wires are present on the square aperture, and the maximum TCS (15.51 cm^2) occurs at a frequency of 4.18 GHz. This frequency corresponds to the resonance frequency of the 3 cm square aperture width. The solid lines labelled "loaded SSA" show the enhanced TCS for 1, 1.5, 2, and 3 GHz when two parallel wires are connected at $d = 1.5$ cm on the SSA.

In Fig. 5(a), the TCS is effectively enhanced to $\approx 3\lambda^2/4\pi$ at 1 and 1.5 GHz using the parallel wires. In Fig. 5(b), the TCS is effectively enhanced to $\approx 3.28\lambda^2/4\pi$ and $3.56\lambda^2/4\pi$ at 2 and 3 GHz, respectively, using the parallel wires. The enhanced TCS for each case is also given in Table II. Table II and Fig. 5 show that the resonance transmissions (either the maximum or enhanced resonance transmissions) of the SSA occur as a result of the loaded capacitive reactances on the electrically SSA.

Moreover, the enhanced TCS is closer to $3\lambda^2/4\pi$ ($G = 1.5$) if the square width is less than $\approx 0.22\lambda$, while the enhanced TCS is closer to $3.56\lambda^2/4\pi$ ($G = 1.78$) if the square width is greater than $\approx 0.22\lambda$. However, when the square width is $\approx 0.22\lambda$, the enhanced TCS is $3.28\lambda^2/4\pi$ ($G = 1.64$), similar to a half-wavelength resonance narrow slot.

As shown in Fig. 5, the resonant frequency can be reduced from 4.18 GHz to various desired frequencies of 1, 1.5, 2, and 3 GHz representing reductions of 76.1, 64.1, 52.2, and 28.2%, respectively, by adding the parallel wires (capacitive reactance).

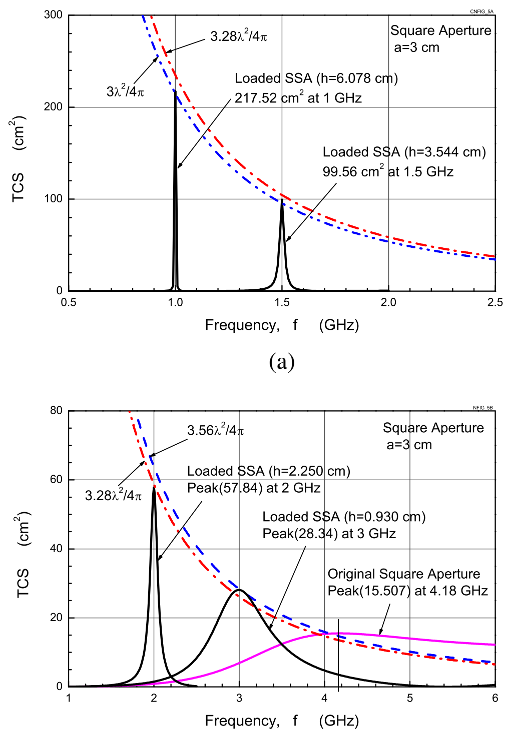

Fig. 5. Transmission cross-sections versus frequency for different wire lengths: $h = 6.087$, 3.544, 2.250, and 0.930 cm connected at the SSA center.

Table II. Enhanced *TCSs* and loading reactances for the resonance transmission

f (GHz)	*TCS* (cm^2)	$G = 1.5$	$G = 1.64$	$G = 1.78$	Parallel wires X_L (Ω)
		$3\lambda^2/4\pi$ (cm^2)	$3.28\lambda^2/4\pi$ (cm^2)	$3.56^2/4\pi$ (cm^2)	
1.0	217.52	214.86	-	-	−152.01
1.5	99.56	95.49	-	-	−243.77
2.0	57.84	-	58.73	-	−359.80
3.0	28.34	-	-	28.33	−748.77

4. Experimental results

To verify the theoretical analysis, experimental results were obtained. Fig. 6 shows a photograph of the experiment setup for measuring the transmission characteristics of the SSA with a two parallel wire loading. A large conducting plane (2×4 m) was attached to a small, square aperture (3×3 cm) in an anechoic chamber. Two parallel copper wires of radius 0.5 mm were connected at the center of the square aperture as a capacitive reactance. Broadband double-ridged horn antennas made by ICU (model No. ICU-MA-04-2, 0.75–6 GHz) were used as the transmitting and receiving antennas. The S-parameters were measured by the antennas under normal incidence and a Wiltron 37225A vector network analyzer. The antennas were placed 100 cm away from the structure to satisfy the far field condition.

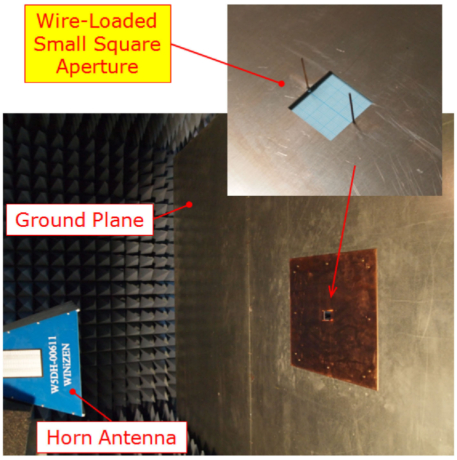

Fig. 6. Photograph of the experiment setup.

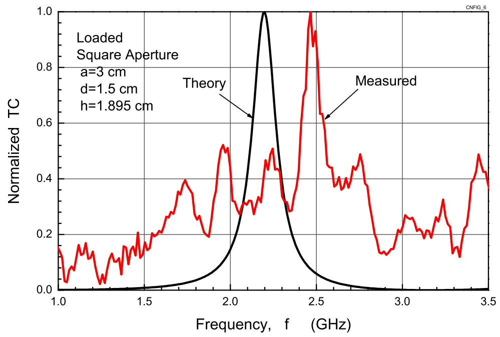

Fig. 7. Calculated and measured frequency characteristics of the transmission coefficient.

The measured and calculated transmission coefficients are shown in Fig. 7. The resonance transmission at a frequency of 2.3 GHz ($h = 1.895$ cm) was examined to confirm the resonance transmission of the SSA by the loading reactance on the aperture. The calculated transmission coefficients were in reasonable agreement with the experimental results, with a $\approx$6% frequency shift. The experimental and theoretical results demonstrate that the resonance transmission of the SSA was effectively enhanced by the parallel wire loading. There were minimal differences and fluctuations in the magnitudes of the measured transmission coefficients. These are mainly caused by fabrication and alignment errors, losses of the large ground plane, and mutual coupling effects between the horn antenna and ground plane.

5. Conclusion

The enhanced resonance transmission (either the maximum or resonance transmissions) of electromagnetic waves through a loaded small square aperture structure on an infinite conducting ground screen was presented. The TCS could be enhanced by adjusting the length of the two parallel wires on the SSA. The maximum or enhanced resonance transmissions occurred as a result of connecting a capacitive reactance to the SSA at a given frequency. When the size of the square aperture was fixed, the enhanced TCS of the SSA with parallel wires was closer to $3\lambda^2/4\pi$ ($G = 1.5$) if the square width was less than $\approx 0.22\lambda$, while the enhanced TCS approached $3.56\lambda^2/4\pi$ ($G = 1.78$) when the square width was greater than $\approx 0.22\lambda$. However, if the square width was $\approx 0.22\lambda$, the enhanced TCS was $3.28\lambda^2/4\pi$ ($G = 1.64$). The enhanced TCS of the SSA by parallel wires has a value between $3\lambda^2/4\pi$ and $3.56\lambda^2/4\pi$.

Acknowledgments

This research was supported by the Basic Science Research Program through the National Research Foundation of Korea (NRF) funded by the Ministry of Education (NRF-2018R1D1A1B07042160 and NRF-2015R1D1A1A09058357).

References

[1] H. A. Bethe: "Theory of diffraction by small holes," Phys. Rev. **66** (1944) 163 (DOI: 10.1103/PhysRev.66.163).

[2] S. B. Cohn: "The electric polarizability of apertures of arbitrary shape," Proc. IRE **40** (1952) 1069 (DOI: 10.1109/JRPROC.1952.273876).

[3] C. J. Bouwkamp: "Theoretical and numerical treatment of diffraction through a circular aperture," IEEE Trans. Antennas Propag. **18** (1970) 152 (DOI: 10.1109/TAP.1970.1139646).

[4] C. M. Butler and K. R. Umashankar: "Electromagnetic excitation of a wire through an aperture-perforated conducting screen," IEEE Trans. Antennas Propag. **24** (1976) 456 (DOI: 10.1109/TAP.1976.1141374).

[5] R. F. Harrington and J. R. Mautz: "A generalized network network formulation for aperture problems," IEEE Trans. Antennas Propag. **24** (1976) 870 (DOI: 10.1109/TAP.1976.1141420).

[6] Y. Rahmat-Samii and R. Mittra: "Electromagnetic coupling through small apertures in a conducting screen," IEEE Trans. Antennas Propag. **25** (1977) 180 (DOI: 10.1109/TAP.1977.1141554).

[7] C. M. Butler, *et al.*: "Electromagnetic penetration through in conducting surfaces," IEEE Trans. Antennas Propag. **26** (1978) 82 (DOI: 10.1109/TAP.1978.1141788).

[8] R. F. Harrington and D. T. Auckland: "Electromagnetic transmission through narrow slots in thick conducting screens," IEEE Trans. Antennas Propag. **28** (1980) 616 (DOI: 10.1109/TAP.1980.1142382).

[9] Y. Naiheng and R. F. Harrington: "Electromagnetic coupling to an infinite wire through a slot in a conducting plane," IEEE Trans. Antennas Propag. **31** (1983) 310 (DOI: 10.1109/TAP.1983.1143025).

[10] R. F. Harrington and J. R. Mautz: "Characteristic modes for aperture problems," IEEE Trans. Microw. Theory Techn. **33** (1985)

500 (DOI: 10.1109/TMTT.1985.1133105).
[11] E. R. Reed and C. M. Butler: "Time-domain electromagnetic penetration through arbitrarily shaped narrow slots in conducting screens," IEEE Trans. Electromagn. Compat. **34** (1992) 161 (DOI: 10.1109/15.155826).
[12] A. El-Hajj and K. Y. Kabalan: "Characteristic modes of a rectangular aperture in a perfectly conducting plane," IEEE Trans. Antennas Propag. **42** (1994) 1447 (DOI: 10.1109/8.320753).
[13] B. A. Lail and S. P. Castillo: "Coupling through narrow slot apertures to thin-wire structures," IEEE Trans. Electromagn. Compat. **42** (2000) 276 (DOI: 10.1109/15.865334).
[14] K.-C. Kim: "Field penetration into a metallic wall with a narrow slot due to nearby dipole source," IEICE Trans. Commun. **E92-B** (2009) 2987 (DOI: 10.1587/transcom.E92.B.2987).
[15] K.-C. Kim, *et al.*: "Shielding effectiveness through narrow slots in dual conducting screens," IEICE Electron. Express **10** (2013) 20130750 (DOI: 10.1587/elex.10.20130750).
[16] K.-C. Kim and Y. K. Cho: "Penetration electric field characteristics of dual plates with narrow slots for the incident plane wave," IEICE Electron. Express **11** (2014) 20141059 (DOI: 10.1587/elex.11.20141059).
[17] K.-C. Kim, *et al.*: "Reduction of electromagnetic penetration through narrow slots in conducting screen by two parallel wires," IEICE Trans. Commun. **E88-B** (2005) 1743 (DOI: 10.1093/ietcom/e88-b.4.1743).
[18] K.-C. Kim: "Aperture cut-off filter for reduction of electromagnetic field penetration through a slot in conducting screens," JKIEES **25** (2014) 1201 (in Korean) (DOI: 10.5515/KJKIEES.2014.25.12.1201).
[19] R. F. Harrington: "Resonant behavior of a small aperture backed by a conducting body," IEEE Trans. Antennas Propag. **30** (1982) 205 (DOI: 10.1109/TAP.1982.1142761).
[20] X. Shi, *et al.*: "Ultrahigh light transmission through a C-shaped nanoaperture," Opt. Lett. **28** (2003) 1320 (DOI: 10.1364/OL.28.001320).
[21] J. Xu, *et al.*: "Design tips of nanoapertures with strong field enhancement and proposal of novel L-shaped aperture," Opt. Eng. **44** (2005) 018001 (DOI: 10.1117/1.1825446).
[22] J. Yeo, *et al.*: "FDTD analysis of resonant transmission in an electrically small circular aperture with a ridge," Proc. IEEE Antennas Propag. Soc. Int. Symp. (2008) 1 (DOI: 10.1109/APS.2008.4619053).
[23] K. W. Kim, *et al.*: "Resonant transmission enhancement with a subwavelength aperture," Proc. IEEE Antennas and Propag. Soc. Int. Symp. (2007) 1521 (DOI: 10.1109/APS.2007.4395796).
[24] S. Xiao, *et al.*: "Enhanced transmission of transverse electric waves through periodic arrays of structured subwavelength apertures," Opt. Express **18** (2010) 6040 (DOI: 10.1364/OE.18.006040).
[25] Y.-K. Cho, *et al.*: "Transmission resonance through small apertures," Proc. Antenna Technology and Applied Electromagnetics (ANTEM) (2012) 1 (DOI: 10.1109/ANTEM.2012.6262311).
[26] F. Miyamaru, *et al.*: "Controlling extraordinary transmission characteristics of metal hole arrays with spoof surface plasmons," Appl. Phys. Lett. **101** (2012) 019901 (DOI: 10.1063/1.4735019).
[27] J.-G. Yoo, *et al.*: "Design and experiment of miniaturized small resonant aperture using modified ridge structure," IEICE Electron. Express **14** (2017) 20170928 (DOI: 10.1587/elex.14.20170928).
[28] Y.-K. Cho, *et al.*: "Experimental verification of electromagnetic scattering via two-dimensional periodic array of small resonant apertures," IEICE Electron. Express **14** (2017) 20170796 (DOI: 10.1587/elex.14.20170796).
[29] K.-C. Kim and Y.-K. Cho: "Resonance transmission of small narrow slots loaded with two parallel wires in a conducting screen," IEICE Electron. Express **15** (2018) 20180015 (DOI: 10.1587/elex.15.20180015).
[30] C. A. Balanis: *Antenna Theory: Analysis and Design* (Wiley, New York, 2005) 3rd ed. Chap. 12.